Simulation of Microseismic Deformation during Hydraulic Fracturing*

S. C. Maxwell[1] and X. Weng[1]

[1]Schlumberger, Calgary, Alberta, Canada (smaxwell@slb.com)

Abstract

Modeled geomechanical deformation associated with hydraulic fracture stimulation of a complex hydraulic fracture provides context for interpretation of microseismic deformation. Partitioning of modeled strains into shear and dilatational components allows relative comparison of the appropriate displacement mode with observed cumulative microseismic moments. A workflow is described where the input parameters of the simulation are varied to match both the footprint and deformation of the microseismicity, which then results in an estimate of the complete fracture network volume and proppant placement. In this way, the effective stimulated volume can be assessed and used as input to a reservoir simulation to investigate well performance and reservoir drainage.

Introduction

Microseismic monitoring is the key technology to image hydraulic fracture stimulation of unconventional reservoirs. Typically, the timing and location of microseismicity is used to interpret the geometry and hydraulic fracture growth. Microseismic waveforms also contain information about the inelastic deformation that can also be used to characterize the hydraulic fracture. However, the detected microseismic activity represents only a portion of the geomechanical deformations associated with the hydraulic fracturing (Maxwell, 2011). In particular, the detected movements are restricted to the time scales corresponding to the bandwidth of the monitoring equipment. Furthermore, in some scenarios at least, the microseismicity corresponds to shear deformations while the hydraulic fracture is generally considered a tensile parting of the rock. Therefore, aseismic deformation comprises an important aspect of the fracture movements beyond what is observed through microseismicity (Maxwell, 2011).

Here, a geomechanical simulation of the hydraulic fracture is used to distinguish the estimated deformation between shear and tensile modes of strain. The observed microseismic deformation as quantified by either the cumulative microseismic moment or displacements can be compared with the appropriate portion of the simulated movements consistent with the deformation mode of the microseismicity. In a particular case study presented here, the microseismicity is interpreted to represent shear deformation and the cumulative seismic moment density is compared to the modeled cumulative shear movements. Validating the shear component of the geomechanics improves the confidence in the entire

simulation, including the estimated tensile opening. This becomes the basis of a workflow using the microseismic deformation to validate the gemechanical fracture network simulation, so that the results can be used to assess the proppant placement and fracture effectiveness and through a reservoir simulation the expected reservoir drainage.

Geomechanical Fracture Network Simulation

The ability to simulate hydraulic fracture growth is a key element of fracture engineering design. Hydraulic fracture stimulations can be modeled through fracture mechanics models that simulate the fracture dilation/strain, leak-off, hydraulic conductivity and associated pressure profile for a given injection volume. Models are commonplace for simple scenarios of relatively planar, 2D fractures. However, in cases of complex fracture networks new methods are only now becoming available with capabilities to address creation of new hydraulic fractures and/or activation of pre-existing natural fractures which GeoConvention 2013: Integration 2 result in coupled geomechanical and hydraulic interaction between individual components of the fracture network (e.g. Weng et al., 2011). Typical input parameters of a complex fracture model are the 1D or 3D stress state and mechanical properties of the rock and pre-existing discrete fracture network (DFN). Cipolla et al., 2010, describes an example of modeling the response of a four-stage hydraulic fracture stimulation of a horizontal Barnett Shale well (Figure 1). In this particular case study, stress variation through the reservoir is believed to have resulted in a change in fracture geometry from relatively narrow, planar fractures for the first two toe stages to a wider, complex fracture network for the final heel stages. A fracture network simulation was created and calibrated to approximate the spatial extent of the microseismicity (Figure 2). Note that it is possible to create a more exact match by modifying the geometry of the input pre-existing fractures.

Deformation Modes

An implicit assumption of the fracture network model is the need to create sufficient fracture volume to accommodate the total injected volume, through fracture dilation. However, dilations within a complex fracture network can also induce shear movements on other fractures, such that the resulting fracture strains will be a combination of shear and tensile dilation. For the fracture model, displacements can be projected as either normal (i.e. tensile or dilational opening) or parallel (i.e. shear) components relative to the fracture orientation. Figure 3 and Figure 4 illustrate these deformation modes in the fracture network shown in Figure 2. Figure 5 and Figure 6 show corresponding contours of the cumulative deformations. Notice that the deformation is in some places predominantly tensile (e.g., segments highlighted with the red arrow) and others mostly shear (e.g. blue arrows). In particular, the single planar fracture in the middle dilates as a mostly tensile deformation mode. The maximum tensile deformation within the network is found to be approximately 3 cm, while the maximum shear deformation is approximately 2 cm.

To compare with the observed microseismicity, a consistent 25 m grid was used to compute both the total modeled and observed deformations. The grid spacing was selected to match the average location uncertainty. In this example, the observed microseismic amplitudes are consistent with the shear radiation patterns of NE-SW or NW-SE strike slip displacements. More generally, seismic moment tensor inversion could also be used to estimate the mode of the microseismic deformation. Based on shear microseismic slippage assumption, contours of the cumulative microseismic moments can be compared with corresponding modeled shear deformations. Beyond the observed microseismic deformations, aseismic deformations are also expected to contribute to the total expected deformation. The seismic efficiency, defined as the ratio of the

radiated seismic energy to the total energy release is also a factor leading to the expectation that microseismic represents only a portion of the total strains. Nevertheless, assuming that these factors are constant through the fracture network, a relative comparison can be made with the microseismicity.

Figure 7 shows contours of the cumulative microseismic moment. These contours are approximately consistent with the modeled shear deformation (Figure 5), although the modeled deformation is more constant through the fracture network where the observed microseismic moment is largest near the treatment well. It is interesting to the note that the relative planar fracture in the middle (arrows in Figure 5 and Figure 7) is relatively low in shear for both the observations and modeling. However, as previously noted the model indicates this fracture is predominantly a tensile opening, which if true would imply a more effective fracture in this region despite the relatively weak microseismicity.

The modeled deformations can be converted to an effective seismic moment by multiplying by the shear modulus and area of each fracture segment. Table 1 compares the total modeled moments for the tensile and shear components and the microseismicity. The tensile component is significantly larger than the shear (about 50x) from the model and the microseismicity is about 0.1% of he modeled shear.

Discussion and Conclusions

In this example, no attempt was made to improve the agreement between the modeled and observed deformations. However, a variable fracture density or alternate fracture properties could be used in the DFN to increase the agreement with observations: both the extent of the microseismicity and the cumulative moment. Alternatively, a series of fracture simulations with various inputs could be generated and the model that matches the relative microseismic deformation could be selected. Improving the match of the appropriate mode of the fracture simulation with the microseismicity, improves the confidence in the overall simulation result. In the example presented here, validating the shear deformation with the microseismicity implies that the dilatational deformation is also valid regardless if the observed microseismicity directly represents tensile opening modes. Fracture dilation is the critical factor for fracture effectiveness providing sufficient fracture volume to accommodate proppant placement, thereby ensuring continued fracture permeability after the stimulation. The model discussed here honors the mass balance of the injected fluid, and can therefore be used to predict the proppant placement within the fracture network. The resulting proppant map can then be used to populate permeability within the fracture network for reservoir simulation of the well performance and reservoir drainage, leading to a better estimate of the effective stimulated volume and reservoir recovery.

References Cited

Cipolla, C.L., M.J. Williams, X. Weng, M. Mack, and S. Maxwell, 2010, Hydraulic Fracture Monitoring to Reservoir Simulation: Maximizing Value: SPE133877.

Maxwell, S.C., 2011, What Does Microseismic Tell Us About Hydraulic Fracture Deformation: Recorder, p. 29-43.

Rich, J.P., and M. Ammerman, 2010, Unconventional Geophysics for Unconventional Plays: SPE 131779.

Weng, X., O. Kresse, C. Cohen, R. Wu, and H. Gu, 2011, Modeling of Hydraulic Fracture Network Propagation in a Naturally Fractured Formation: SPE140253.
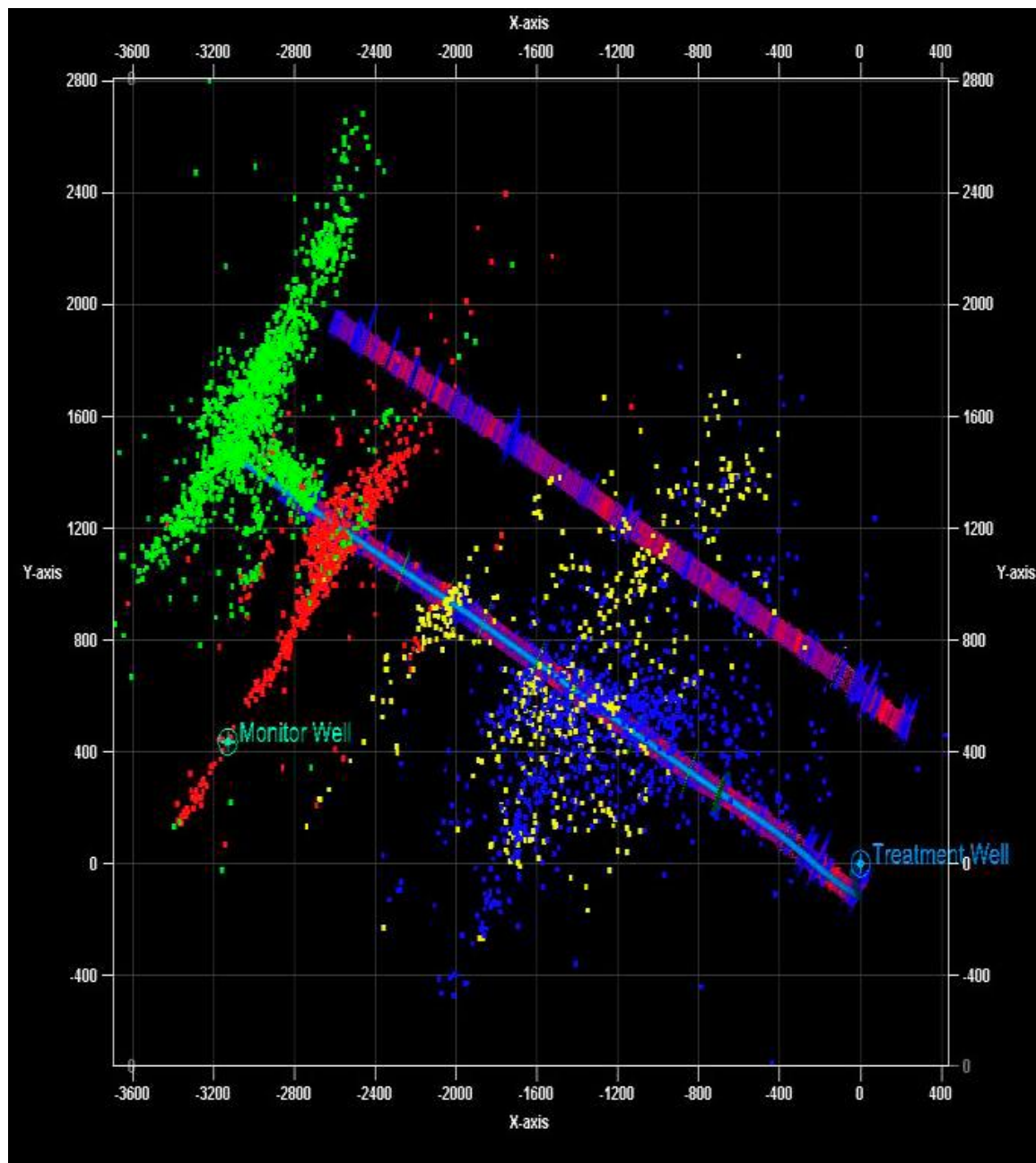
Figure 1. Map view of a four-stage hydraulic fracture stimulation in the Barnett Shale (Rich and Ammerman, 2010).
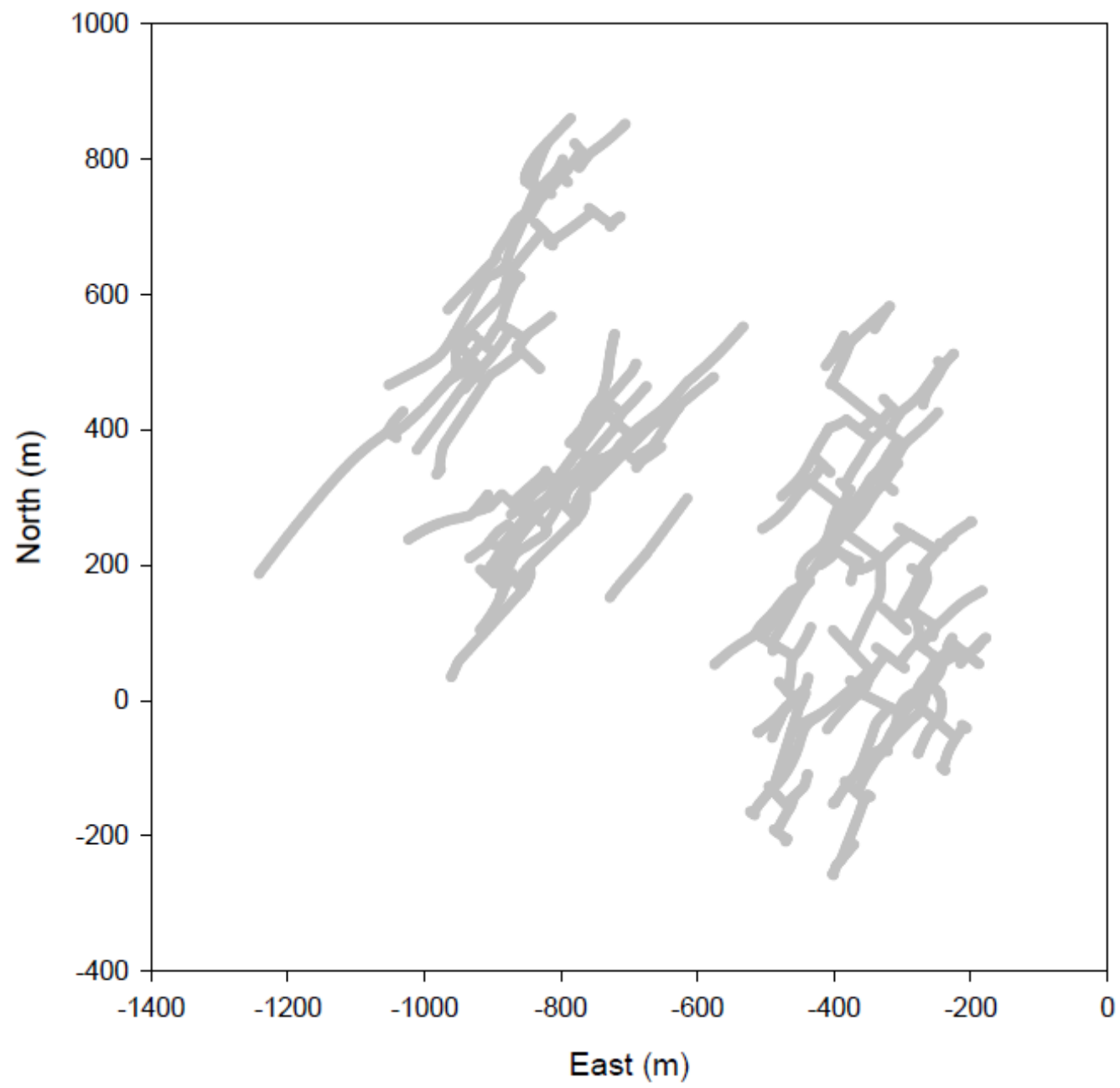
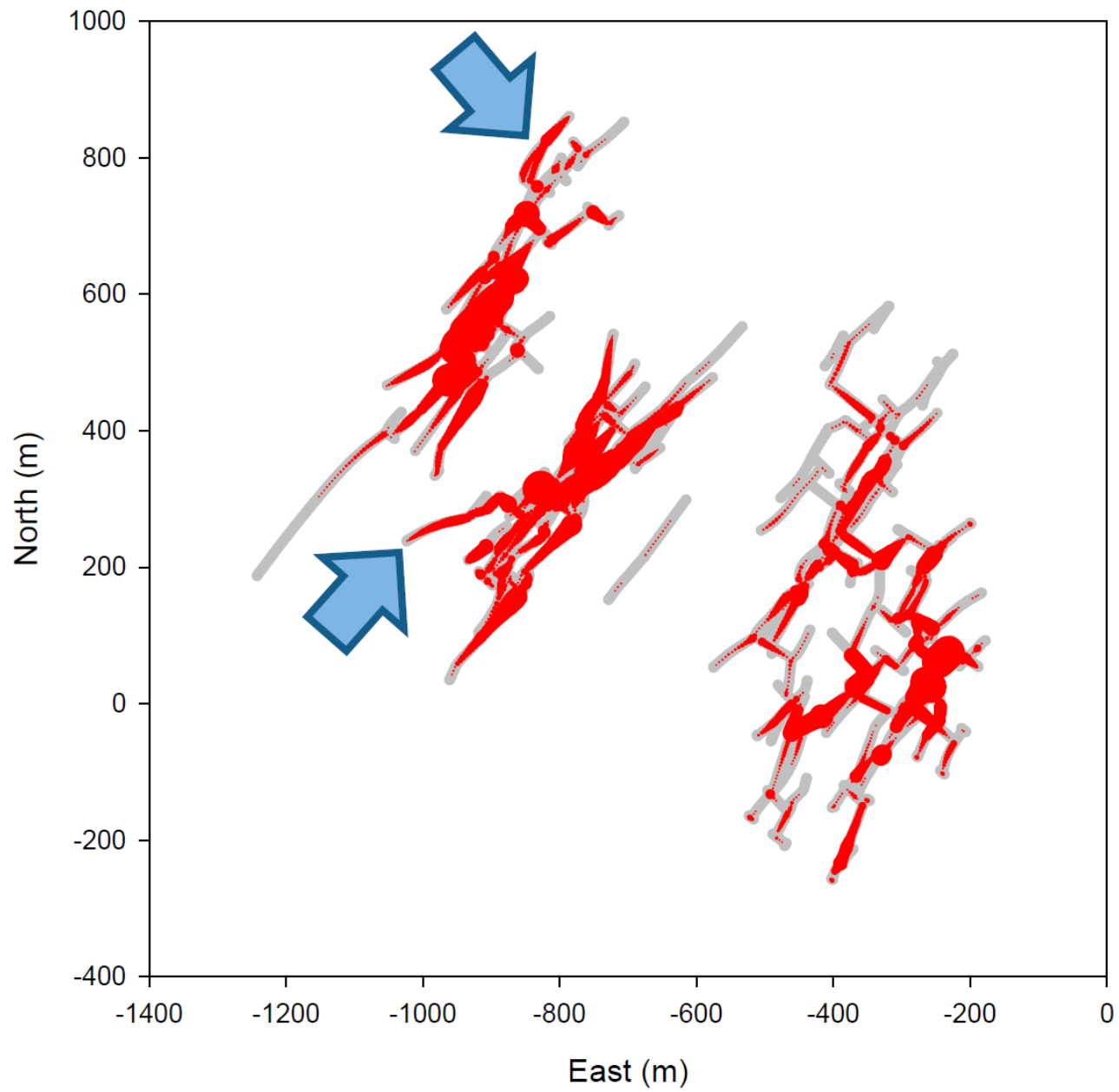Figure 2. Fracture network segments approximating the extent of the microseismicity.

Figure 3. Modeled shear deformations with symbol diameter proportional to shear displacement (maximum 0.02 m). Blue arrows indicate two regions with significant shearing.
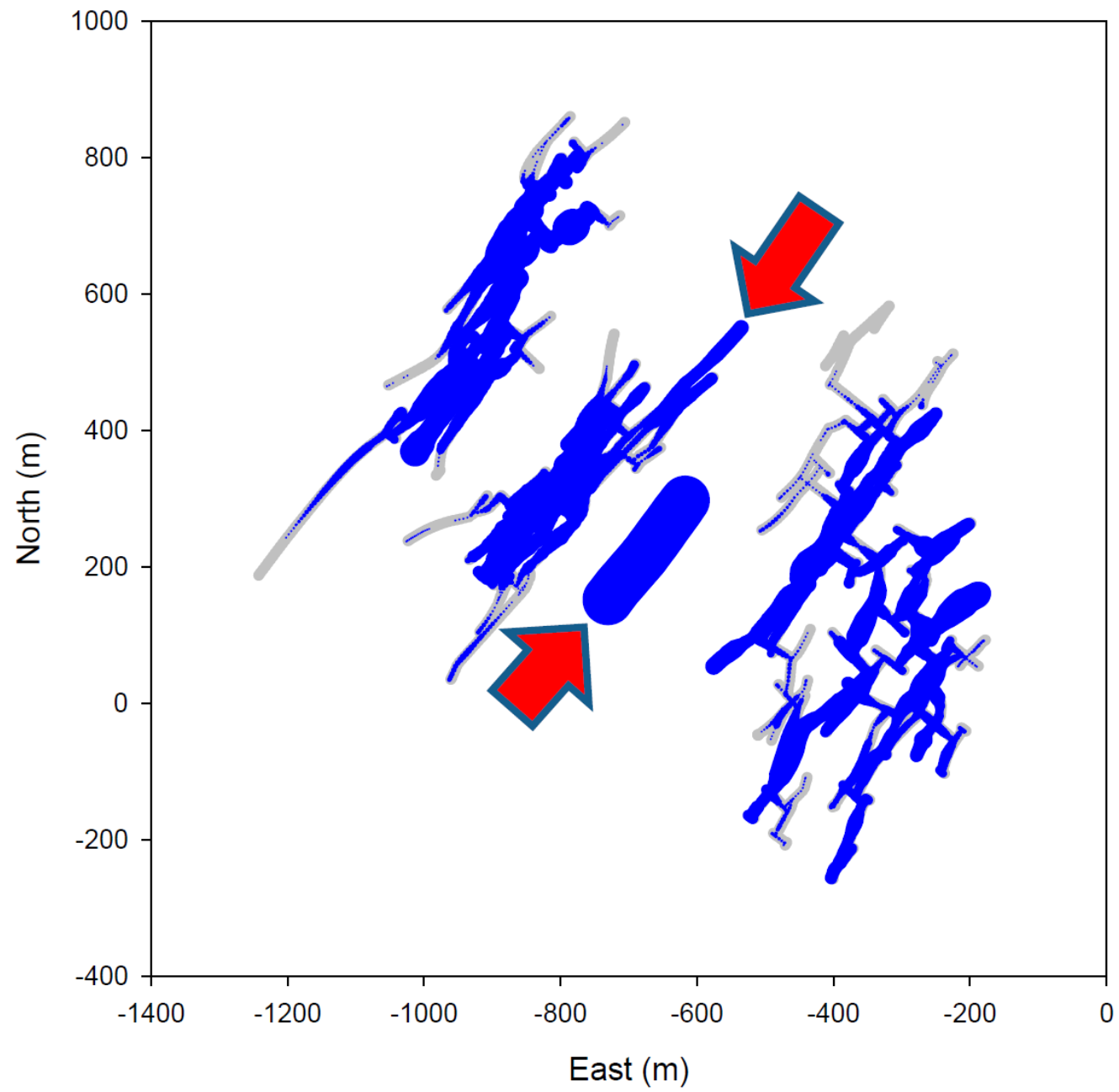
Figure 4. Modeled tensile deformation (maximum 0.03 m). Red arrows indicate two regions with significant dilation.
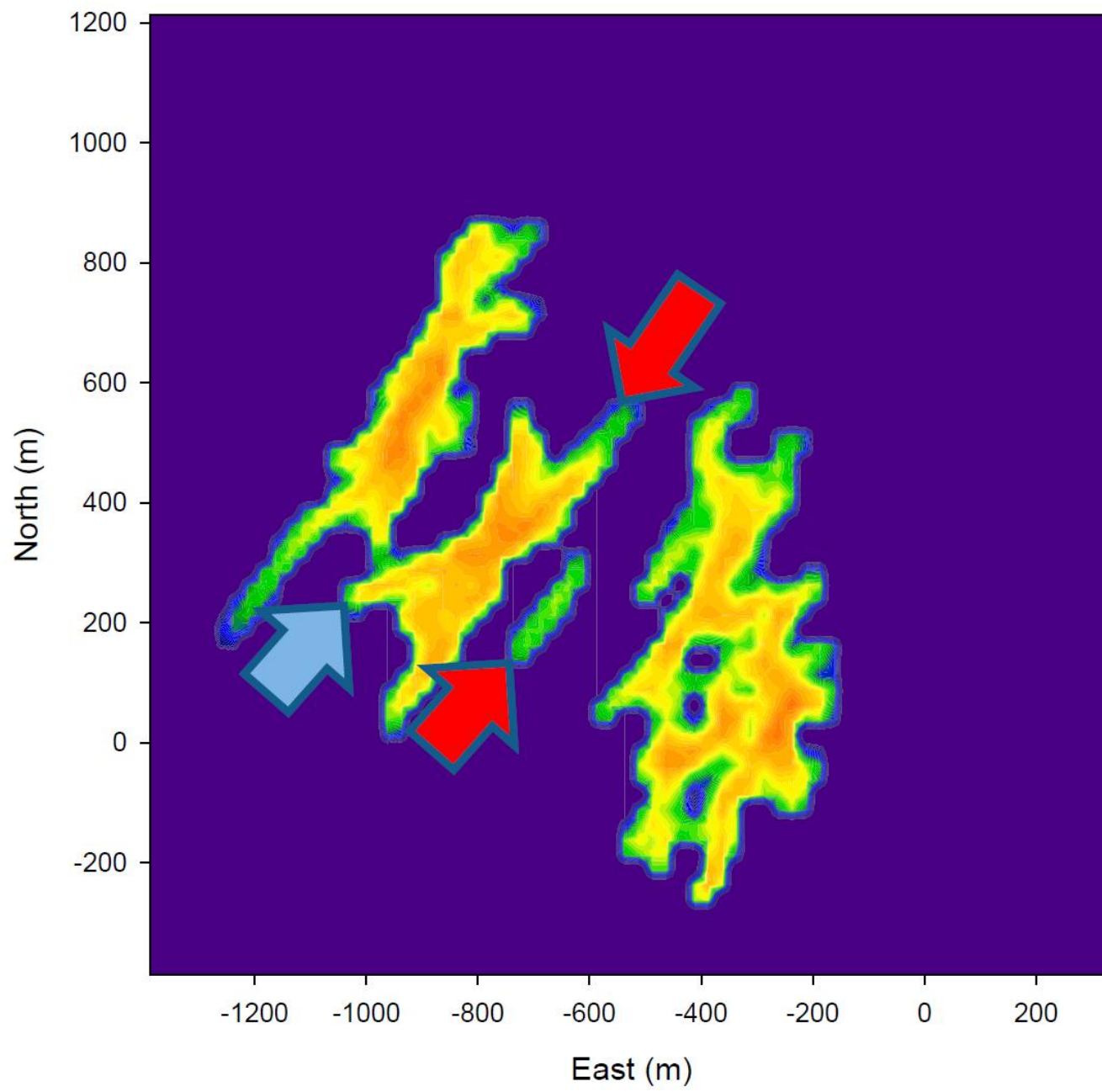
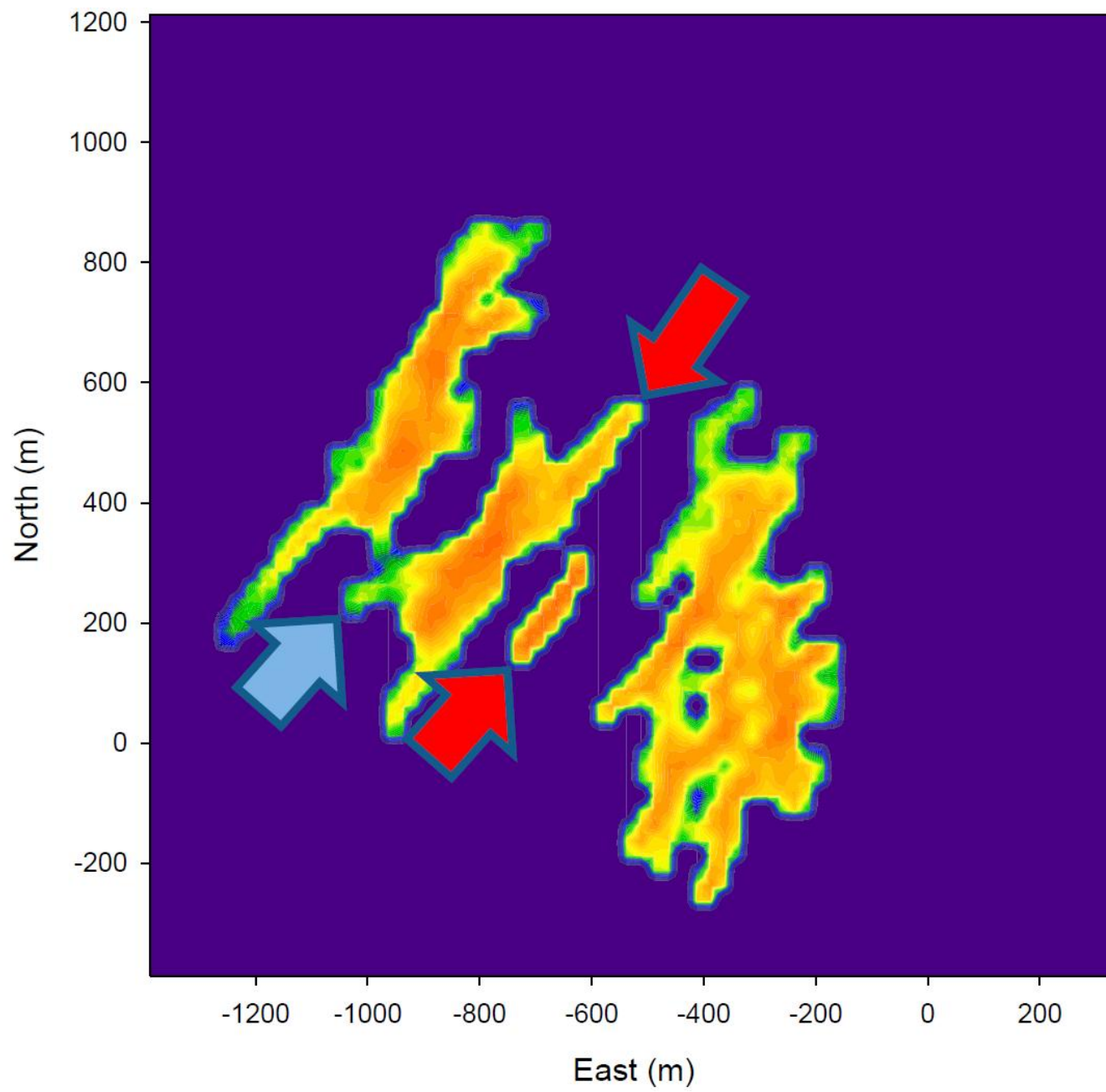Figure 5. Contours of log of total modeled shear deformation.

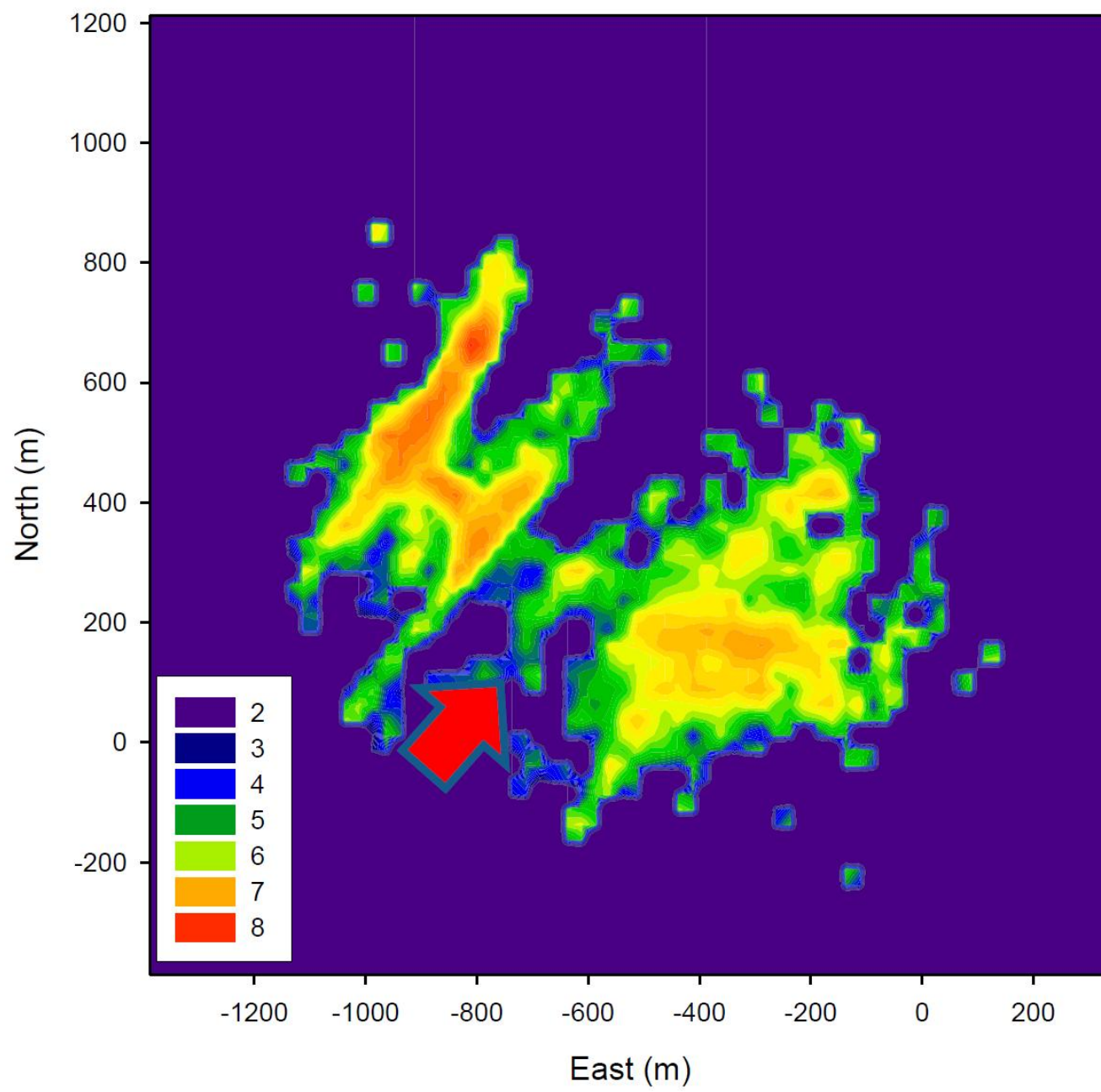Figure 6. Contours of log of modeled tensile deformation.

Figure 7. Contours of log of cumulative seismic moment.

Total Modeled Shear Moment	Total Modeled Tensile Moment	Total Microseismic Moment
3.18e12 Nm	1.65e14 Nm	3.13e9 Nm

Table 1. Comparison of the total modeled moments for the tensile and shear components and the microseismicity.